

Impedance Modulation for Negotiating Control Authority in a Haptic Shared Control Paradigm

Vahid Izadi¹, Akshay Bhardwaj², and Amir H. Ghasemi¹

Abstract—Communication and cooperation among team members can be enhanced significantly with physical interaction. Successful collaboration requires the integration of the individual partners’ intentions into a shared action plan, which may involve a continuous negotiation of intentions and roles. This paper presents an adaptive haptic shared control framework wherein a human driver and an automation system are physically connected through a motorized steering wheel. By virtue of haptic feedback, the driver and automation system can monitor each other actions and can still intuitively express their control intentions. The objective of this paper is to develop a systematic model for an automation system that can vary its impedance such that the control authority can transit between the two agents intuitively and smoothly. To this end, we defined a cost function that not only ensures the safety of the collaborative task but also takes account of the assistive behavior of the automation system. We employed a predictive controller based on modified least square to modulate the automation system impedance such that the cost function is optimized. The results demonstrate the significance of the proposed approach for negotiating the control authority, specifically when humans and automation are in a non-cooperative mode. Furthermore, the performance of the adaptive haptic shared control is compared with the traditional fixed automation impedance haptic shared control paradigm.

I. INTRODUCTION

Haptic shared control is an emerging research topic with a wide range of applications in the areas such as smart manufacturing, autonomous driving, rehabilitation, health-care, education, and training [1]–[11]. Traditionally, interactive robots were designed to act mainly as reactive followers where the robot (with some level of autonomy) followed the human’s commands [12]–[14]. However, this type of master-servant arrangement does not capture the sense of partnership [15]–[17] that we mean when we speak of two humans cooperatively moving a piece of furniture. A robot as a pro-active partner, also called a co-robot, should be capable of monitoring human actions, as well as communicating its behavior, and even negotiating and exchanging roles with a human partner [18], [19]. These criteria give rise to a set of fundamental questions that we aim to answer in this research. For instance, (1) what are the interaction models between a human and co-robot in a Haptic Shared Control framework? (2) Knowing the interaction models, how should a co-robot facilitate exchanging roles dynamically? (3) What strategies

should a co-robot take to create consensus with a human while also guaranteeing the safety and performance of the task? Moreover, (4) how may uncertainty in the behavior of the human-operator affect these interaction models and consensus models?

To seamlessly combine the commands of a human operator and automation system, most of the existing efforts have been devoted to designing an interface so that the human’s high-level commands (human’s intentions) can be exploited. Specifically, in the context of physical human-robot interaction, force/torque sensors are embedded in the haptic interface for recognizing human intentions and consequently adjusting the robot’s behavior. However, when the automation system and human operator simultaneously interact with each other (especially in an uncertain environment), the force sensors measurements are insufficient for determining the human’s intents. To resolve this issue, we propose to measure the human’s impedance (stiffness of the muscles) as a potential indicator for determining how a human operator dynamically exchanges his role (leader/follower) within a collocative task. We argue if the roles of the two agents are agreed upon, then an appropriately timed nudge from one agent can be interpreted by the other and followed or optionally hindered.

To solve an optimal control problem, several methods exist such as least squares (LS), linear programming (LP), and quadratic programming (QP). The constraints on the control signal or the states play the main role in the solutions of such problems. In this paper, to achieve a non-negative value for the automation’s impedance with a computationally inexpensive method, a modified version of least squares is provided.

The outline of this paper is as follows. Section II presents the basics of adaptive haptic shared control paradigm. Section III presents the basics of a controller that adaptively modulate the automation’s impedance. Section IV presents numerical results followed by Section V which presents the conclusions and future work.

II. ADAPTIVE HAPTIC SHARED CONTROL FRAMEWORK

Figure 1 shows a schematic of an adaptive haptic shared control. Three entities each impose a torque on the steering wheel: a human driver through his hands, an automation system through a motor, and the road through the steering linkage. The driver model consists of a cognitive controller, coupled with a biomechanics subsystem. In Figure 1, θ_H represents the drivers intent, which is an output of the cognitive controller. Impedance Z_H represents the biomechanics of the

¹ Vahid Izadi and Amir H. Ghasemi are with the Department of Mechanical Engineering, the University of North Carolina at Charlotte, Charlotte, NC, 28223, vizadi@uncc.edu, ah.ghasemi@uncc.edu

² Akshay Bhardwaj is with the Department of Mechanical Engineering, University of Michigan, Ann Arbor, MI, 48109, akshaybh@umich.edu

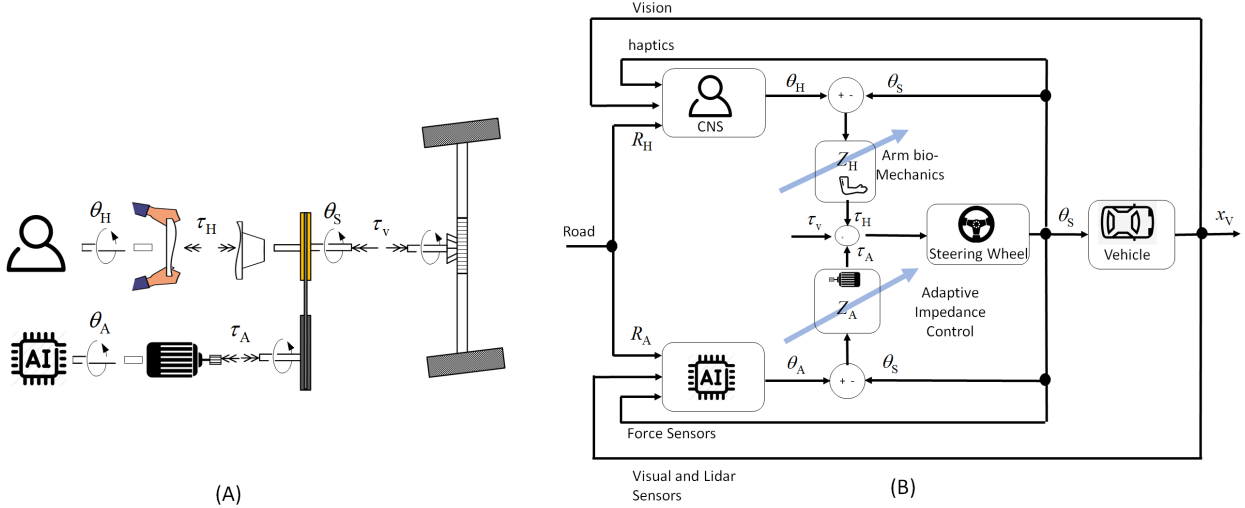


Fig. 1. (A) A general model of control sharing between driver and automation. (B) A block diagram is laid out to highlight the interaction ports between subsystems.

driver's arm, which is backdriveable (the driver impedance is not infinite). To indicate that driver impedance varies with changes in grip on the steering wheel, use of one hand or two, muscle co-contraction, or posture changes, we have drawn an arrow through Z_H . In this paper, the driver and automation system are both shown with a similar structure. Specifically, the automation system is modeled as a higher-level controller (AI) coupled with a lower-level impedance controller. The focus of this paper is on the design of a backdrivable impedance Z_A . That is, the automation is not designed to behave as an ideal torque source. Rather, the automation imposes its command θ_A through an impedance Z_A , which can be varied under control of the automation to express the automation's current level of control authority. Furthermore, the reference signals R_H and R_A represent the goals of the driver and the automation system, respectively. It should be noted that these goals may not necessarily be the same, which is when the negotiation of control authority becomes important. From the model presented in Figure 1, it follows that the position of the steering wheel θ_S is a function of the humans intent θ_H , automations intent θ_A , and the road feedback torque τ_V that results from the forces arising on the steering rack due to tire-road interaction [20]. For a certain impedance, the steering wheel angle is

$$\theta_{SW}(s) = \frac{Z_H(s)\theta_H(s) + Z_A(s)\theta_A(s) + \tau_V(s)}{J_{eq} + B_{SW}s + Z_H(s) + Z_A(s)} \quad (1)$$

where $J_{eq} = J_{SW} + J_H + J_A$, where J_{SW} is the steering wheel inertia, J_H is the inertia of human's hand and J_A is the inertia of automation motor [4], [8].

It follows from (1) by changing his/her impedance (increasing Z_H by co-contracting muscles), the human driver can increase his control authority. Likewise, the automation can be designed such that by imposing higher impedance, and it requests a higher control authority. In this paper, we define the level of authority as a relationship between the

human's impedance and automation's impedance.

To present how impedance may evolve in time, we introduce the following dynamic models:

$$\dot{Z}_H(t) = \alpha_H Z_H(t) + \beta_H \Gamma_H(t) \quad (2)$$

$$\dot{Z}_A(t) = \alpha_A Z_A(t) + \beta_A \Gamma_A(t) \quad (3)$$

where $Z_H = [B_H \ K_H]^T$ and K_H and B_H are the stiffness and damping associated with humans' biomechanics; $Z_A = [B_A \ K_A]^T$ and K_A and B_A are the stiffness and damping associated with the motor's lower-level proportional-derivative controller; $\Gamma_H = [\Gamma_{bH}(t) \ \Gamma_{kH}(t)]^T$ is the humans control action for modulating his impedance and $\Gamma_A = [\Gamma_{bA}(t) \ \Gamma_{kA}(t)]^T$ is the automations control input for modulating its impedance. Additionally,

$$\alpha_H = \begin{bmatrix} \alpha_{bH} & 0 \\ 0 & \alpha_{kH} \end{bmatrix}, \quad \beta_H = \begin{bmatrix} \beta_{bH} & 0 \\ 0 & \beta_{kH} \end{bmatrix} \\ \alpha_A = \begin{bmatrix} \alpha_{bA} & 0 \\ 0 & \alpha_{kA} \end{bmatrix}, \quad \beta_A = \begin{bmatrix} \beta_{bA} & 0 \\ 0 & \beta_{kA} \end{bmatrix} \quad (4)$$

where $\{\alpha_{bH}, \alpha_{kH}, \alpha_{bA}, \alpha_{kA}, \beta_{bH}, \beta_{kH}, \beta_{bA}, \beta_{kA}\}$ are constant parameters. This formulation captures how impedance evolves in time. Ideally, to determine an optimal behavior for the automation system, optimization should be performed over all control signals of the automation system (i.e., θ_A, Γ_A). However, the focus of this paper is to determine Γ_A as means for allocating the level of authority between the driver and the automation system.

III. IMPEDANCE MODULATION CONTROLLER DESIGN

In this section, we present a predictive controller for modulating the automation impedance such that the assistive behavior of the automation system improves while the safety of the task is also guaranteed.

The discrete-time model of the impedance dynamics (2)

and (3) using the Forward Euler method would be

$$Z_H(k+1) = \tilde{\alpha}_H Z_H(k) + \tilde{\beta}_H \Gamma_H(k+1) \quad (5)$$

$$Z_A(k+1) = \tilde{\alpha}_A Z_A(k) + \tilde{\beta}_A \Gamma_A(k+1) \quad (6)$$

where $\tilde{\alpha}_H = (I - T_s \alpha_H)^{-1}$, $\tilde{\beta}_H = \tilde{\alpha}_H T_s \beta_H$, $\tilde{\alpha}_A = (I - T_s \alpha_A)^{-1}$, $\tilde{\beta}_A = \tilde{\alpha}_A T_s \beta_A$, and T_s is the sampling time.

Now let us define the vector $\Theta_i(k) = [\dot{\theta}_i(k) \ \theta_i(k)]$ where $i \in \{\text{SW}, \text{H}, \text{A}\}$. Note that

$$\dot{\theta}_i(k) = \frac{\theta_i(k) - \theta_i(k-1)}{T_s} \quad (7)$$

Next, let us define a cost function $J(k)$ in the form of

$$\begin{aligned} \min_{\Gamma_A} J(k) = & \sum_{j=k+1}^{k+N_p} \{ \|Z_H(j)^T \Theta_H(j)^T + Z_A(j)^T \Theta_A(j)^T\| \\ & - \varepsilon(j) \| + \|Z_H(j)^T \Theta_H(j)^T - Z_A(j)^T \Theta_A(j)^T\| \} \end{aligned} \quad (8)$$

The first term of the cost function is to ensure safe steering. Specifically, we define ε as a minimum required torque that can guarantee the safe maneuver. In this paper, we assume ε is known. The second term of the cost function is to minimize the disagreement between a human driver and the automation system. The steering angle, θ_S and its rate of change $\dot{\theta}_S$ can be directly measured from the sensor. Further, we assume that Z_H and Θ_H are known and can be measured.

The goal in the cost function is to determine Γ_A such that the cost function J is minimized. To this end, $Z_A^T \Theta_A^T$ can be presented as

$$Z_A(k)^T \Theta_A(k)^T = B_A(k) \left[\frac{\theta_A(k) - \theta_A(k-1)}{T_s} \right] + K_A(k) \theta_A(k) \quad (9)$$

Eq. 9 can be rewritten as

$$Z_A(k)^T \Theta_A(k)^T = (\Phi(k) + \Psi(k)) \begin{bmatrix} \theta_A(k) \\ \theta_A(k-1) \end{bmatrix}, \quad (10)$$

where

$$\Phi(k) = \tilde{\alpha}_A \left[\frac{B_A(k-1)}{T_s} + K_A(k-1) \quad -\frac{B_A(k-1)}{T_s} \right] \quad (11)$$

$$\Psi(k) = \tilde{\beta}_A \left[\frac{\Gamma_{BA}(k)}{T_s} + \Gamma_{KA}(k) \quad -\frac{\Gamma_{BA}(k)}{T_s} \right] \quad (12)$$

The Φ and Ψ represent modified mechanical impedance and control action vectors, respectively. By propagating the automation torque for the next time steps until N_p step, the Φ and Ψ vectors will move forward in the time. Let us create the prediction matrices for N_p steps. From Equation (10), we obtain the following $Z_A(k+1)^T \Theta_A(k+1)^T$ for step $(k+1)$

$$\begin{aligned} Z_A(k+1)^T \Theta_A(k+1)^T = & (\tilde{\alpha}_A [\Phi(k) + \Psi(k)] \\ & + \Psi(k+1)) \begin{bmatrix} \theta_A(k) \\ \theta_A(k-1) \end{bmatrix} \end{aligned} \quad (13)$$

Propagating further to $(k+N_p)$ index we obtain

$$\begin{aligned} Z_A(k+N_p)^T \Theta_A(k+N_p)^T = & ((\tilde{\alpha}_A)^{N_p} [\Phi(k) + \Psi(k)] \\ & + (\tilde{\alpha}_A)^{N_p-1} \Psi(k+1) + \dots + \Psi(k+N_p)) \begin{bmatrix} \theta_A(k) \\ \theta_A(k-1) \end{bmatrix} \end{aligned} \quad (14)$$

The prediction matrix $Z_A^T \Theta_A^T$ can then be written as follows

$$Z_A^T \Theta_A^T = \bar{\Theta} \Omega(\Phi, \Psi), \quad (15)$$

where

$$\begin{aligned} Z_A^T \Theta_A^T = & \begin{bmatrix} Z_A(k+N_p)^T \Theta_A(k+N_p)^T \\ \vdots \\ Z_A(k+1)^T \Theta_A(k+1)^T \\ Z_A(k)^T \Theta_A(k)^T \end{bmatrix} \quad (16) \\ \bar{\Theta}^T = & \begin{bmatrix} \Theta_A(k+N_p) & \dots & 0 & 0 \\ \Theta_A(k+N_p-1) & \dots & 0 & 0 \\ \vdots & \ddots & \vdots & \vdots \\ 0 & \dots & \Theta_A(k+1) & 0 \\ 0 & \dots & \Theta_A(k) & 0 \\ 0 & \dots & 0 & \Theta_A(k) \\ 0 & \dots & 0 & \Theta_A(k-1) \end{bmatrix} \quad (17) \end{aligned}$$

$\Omega(\Phi, \Psi) =$

$$\begin{bmatrix} \left\{ \tilde{\alpha}_A^{N_p} [\Delta(k)] + \tilde{\alpha}_A^{N_p-1} \Psi(k+1) + \dots + \Psi(k+N_p) \right\}^T \\ \vdots \\ \left\{ \tilde{\alpha}_A [\Delta(k)] + \Psi(k+1) \right\}^T \\ \left\{ \Delta(k) \right\}^T \end{bmatrix} \quad (18)$$

where $\Delta(k) = \Phi(k) + \Psi(k)$.

According to the second term of (8), in the ideal model, the value of $Z_H^T \Theta_H^T$ will be equal to $Z_A^T \Theta_A^T$. On the other hand, in (16), the amount of automation control action at a time step k can be determined by using methods like linear programming (LP), quadratic programming (QP) and least square (LS). As it can be seen in the (16), the solution from the optimal solver will give us the summation of Φ and Ψ . In the LP, QP, and LS methods, it is possible to have a negative value. This means, the mechanical link on the automation side is disconnected (has zero impedance). In this paper, a modified version of the LS method is used to solve the cost function with a non-negative solution (non-negative impedance). The modified least-square is an LS optimization problem which is subjected to non-negativity constraints. The procedure to implement these constraints is to solve the corresponding unconstrained LS problem and then overwrite any negative values with zeros.

IV. RESULTS

In this section, we present a series of simulation results to show the effectiveness of the proposed adaptive haptic shared

control (HSC) for improving the collaboration between the human driver and the automation system. We specifically consider two modes of interactions: cooperative and non-cooperative. A cooperative mode is when R_H and R_A (see Fig. 1) have the same sign and non-cooperative mode is when the sign of R_H and R_A is different. In this paper, we assume θ_H and θ_A , which are the outputs of a higher-level controller (e.g., MPC-based controller) are known and given. We aim to determine an optimal Γ_A such that the cost function J defined in (8) is minimized. For all the simulation results presented below, the steering wheel inertia is $J_{SW} = 0.1$ N.m/rad/s² and damping coefficient for the steering wheel is $B_{SW} = 0.01$ N.m/rad/s. Also, the human's hand inertia is $J_H = 0.001$ N.m/rad/s² [21] and the motor inertia is $J_A = J_H$. The sampling time is $T_s = 0.1$ second and the control and estimation horizon is $N_p = 20$. The matrices α_H , α_A , β_H , and β_A defined in Equation (4) are all assumed to be identity matrices. The road torque feedback τ_V is assumed to be zero.

Figure 2 demonstrates a cooperative mode of interaction between a human driver and an automation system when both driver and automation intentions have the same sign ($\text{sgn}(\theta_H) = \text{sgn}(\theta_A)$). The human's impedance parameters are shown with red dashed lines. We consider a scenario where the human's stiffness is adaptively changing through time. Specifically, the initial value of stiffness K_H is 1 N.m/rad and at $t = 8$ and $t = 20$ seconds and it changes from 1 N.m/rad to 0.05 N.m/rad and from 0.05 N.m/rad to 0.75 N.m/rad, respectively. The damping is held fixed at $B_H = 0.01$ N.m/rad/s. The Figure 2-c shows that automation tries to match its impedance with the human driver in the cooperative task.

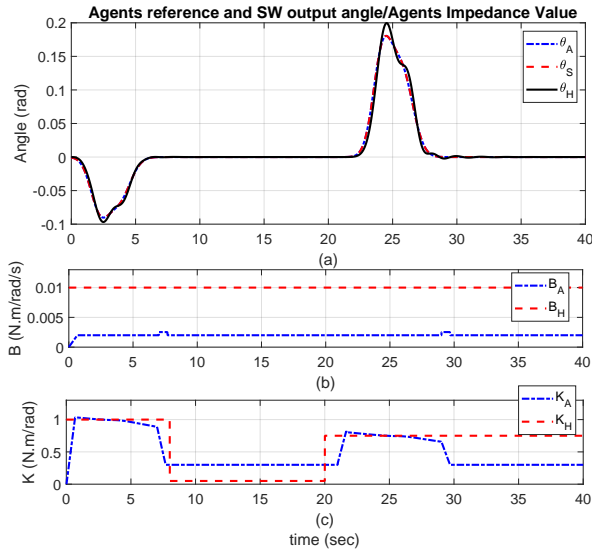


Fig. 2. Cooperative mode of integration between a human driver and an automation system with adaptive HSC.

Figure 3 demonstrate a non-cooperative mode of interaction between a human driver and an automation system when the driver and automation intentions have different

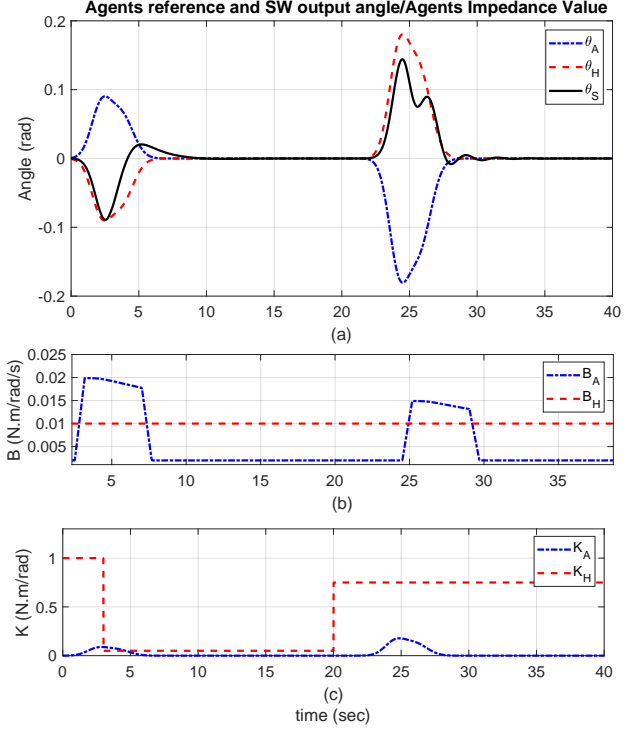


Fig. 3. Non-cooperative mode of integration between a human driver and an automation system with adaptive HSC.

signs ($\text{sgn}(\theta_H) \neq \text{sgn}(\theta_A)$). The initial value of stiffness K_H is 1 N.m/rad and at $t = 3$ and $t = 20$ seconds and it changes from 1 N.m/rad to 0.05 N.m/rad and from 0.05 N.m/rad to 0.75 N.m/rad, respectively. The damping is held fixed at $B_H = 0.01$ N.m/rad/s. Similar to Figure 2, the human's impedance dynamically changes with time. However, to reduce the disagreement between the two agents, the automation system adopts a smaller stiffness. While automation damping B_A also remains low it still changes at the instances of conflict. We are currently investigating the reason behind the variation in damping.

Figure 4 shows how different values of ε may affect the steering angle as well as the differential torque (fight between the two agents) in the non-cooperative mode. By selecting higher values for ε the minimum torque required for the safe maneuver is required which results in a bigger differential torque. To ensure the minimum required input for the safe maneuver, there will be a minimum fight between the human and automation system. The amount of fight increases as the amount of minimum required torque increases.

Next, we compare the performance of a non-adaptive (when the automation impedance does not change as the human's impedance changes) haptic shared control paradigm with an adaptive haptic shared control paradigm in the case of a non-cooperative mode of interaction between the driver and automation. Considering $\varepsilon = .1$, (d), (e) and (f) plots of Fig 5 present the impedance and steering angle with impedance modulation (adaptive), while (a), (b) and (c) shows them without impedance modulation (non-adaptive). It follows from Fig 5 that in non-adaptive mode, the driver's

and automation's control command cancels out, and the steering wheel is almost zero ($\theta_S \approx 0$). However, this issue seems to be solved in adaptive haptic shared control. Additionally, the disagreement between the two agents in the adaptive haptic shared control paradigm is much lower than the non-adaptive haptic mode.

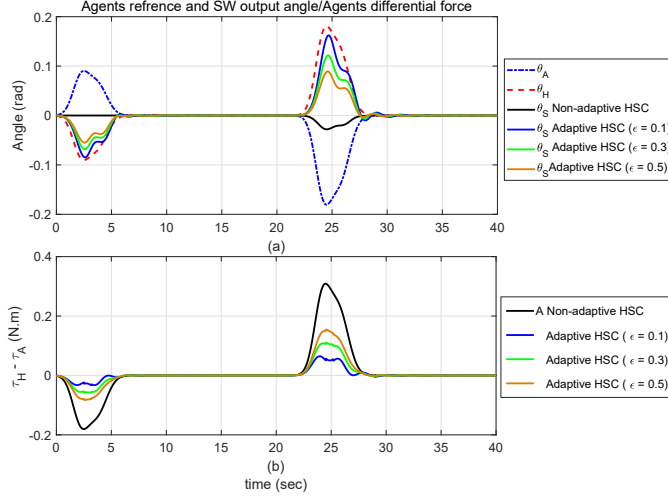


Fig. 4. The effect of different values of ϵ (a) on the steering wheel angle and (b) on the differential torque (conflict) between human and automation.

V. CONCLUSIONS AND FUTURE WORK

This paper presents the principles of the adaptive haptic shared control paradigm. Specifically, we introduce the impedance modulation as one possible mechanism for negotiation of the control authority. We propose a predictive control approach where the impedance of an automation system is modulated so that the fight between the two agents is minimized while the safety of the system is guaranteed. In the future, we plan to extend the outcomes of this research to experimental studies. To this end, we have developed a low-fidelity fixed-base driving simulator (see Fig. 6). The simulator features a steering wheel that is motorized and a screen that displays a virtual driving environment. The steering wheel is further equipped with a force sensor that is within easy reach of driver's hands.

So far, we have assumed that driver intent θ_H and driver impedance Z_H are available. However, in an actual driving experiment, we would need to estimate these parameters online. In the past, it has been shown that the grip force can be used as a proxy to estimate the driver impedance [22], [23]. Accordingly, in our driving experiments in the future, we plan to use the grip force sensor measurements to estimate the human's impedance on the fly. Additionally, to have an approximate estimate of the human's intent θ_H , we plan to ask the participants to follow a pre-designed path. By integrating this online information about the human's intention (known from a pre-designed path), human's estimated impedance (known from the force sensor), and the automation's intentions (AI's output), we intend to test the

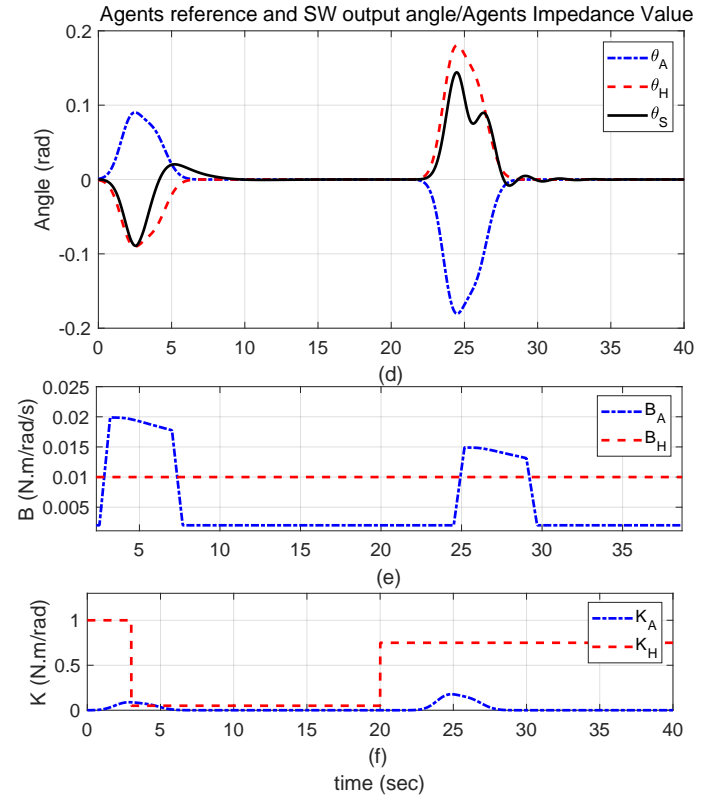
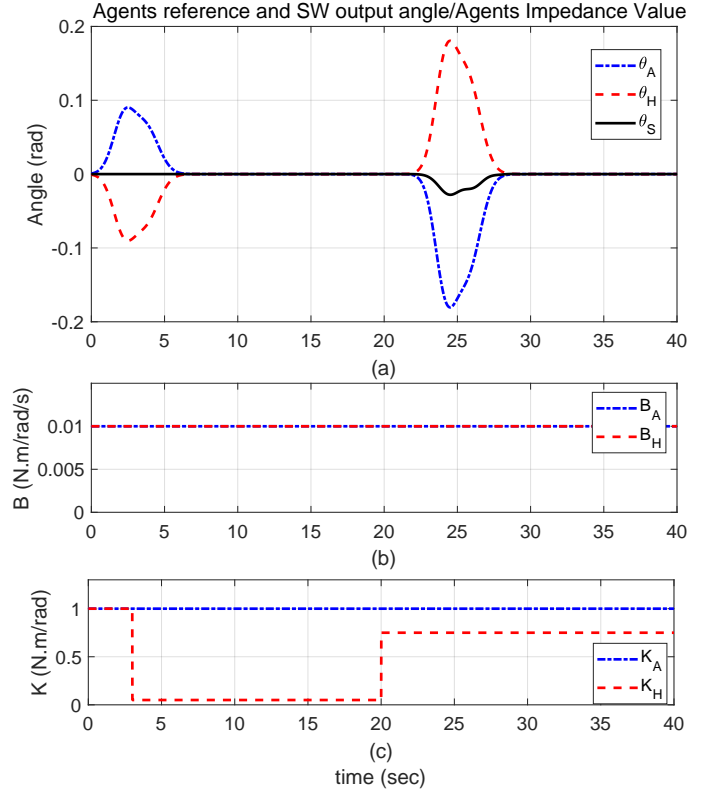


Fig. 5. Comparison between adaptive and non-adaptive haptic shared control paradigms. Figures (a) to (c) show the reference angle and impedance parameters for the non-adaptive (fixed impedance) haptic shared control paradigm and (d) to (f) show the reference angle and impedance parameters for the adaptive haptic shared control paradigm.

performance of the proposed adaptive haptic shared control paradigm on the actual hardware.

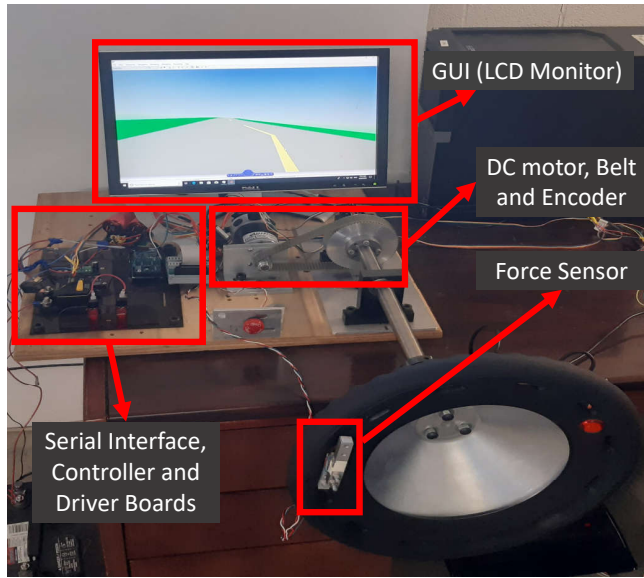


Fig. 6. Fixed base driving simulator: experimental setup.

REFERENCES

- [1] Arvin Agah. Human interactions with intelligent systems: research taxonomy. *Computers & Electrical Engineering*, 27(1):71–107, 2000.
- [2] A Albu-Schaffer, Antonio Bicchi, G Boccadamo, R Chatila, A De Luca, A De Santis, G Giralt, G Hirzinger, V Lippiello, R Mattone, et al. Physical human-robot interaction in anthropic domains: safety and dependability. In *Proceeding 4th IARP/IEEE-EURON Workshop on Technical Challenges for Dependable Robots in Human Environments*, 2005.
- [3] Pieter Beyl, K Knaepen, S Duerinck, Michaël Van Damme, Bram Vanderborght, R Meeusen, and Dirk Lefeber. Safe and compliant guidance by a powered knee exoskeleton for robot-assisted rehabilitation of gait. *Advanced Robotics*, 25(5):513–535, 2011.
- [4] Paul Boehm, Amir H Ghasemi, Sile O’Modhrain, Paramsothy Jayakumar, and R Brent Gillespie. Architectures for shared control of vehicle steering. *IFAC-PapersOnLine*, 49(19):639–644, 2016.
- [5] Amir H Ghasemi, Mishel Johns, Benjamin Garber, Paul Boehm, Paramsothy Jayakumar, Wendy Ju, and R Brent Gillespie. Role negotiation in a haptic shared control framework. In *Adjunct Proceedings of the 8th International Conference on Automotive User Interfaces and Interactive Vehicular Applications*, pages 179–184. ACM, 2016.
- [6] Amir H. Ghasemi and Hossein Rastgoftar. Adaptive haptic shared control framework using markov decision process. In *Dynamic Systems and Control Conference (DSCC), 2018*. ASME, 2018.
- [7] Amir H. Ghasemi. Game theoretic modeling of a steering operation in a haptic shared control framework. In *Dynamic Systems and Control Conference (DSCC), 2018*. ASME, 2018.
- [8] Amir H Ghasemi, Paramsothy Jayakumar, and R Brent Gillespie. Shared control architectures for vehicle steering. *Cognition, Technology & Work*, pages 1–11, 2019.
- [9] Nicola Vitiello, Tommaso Lenzi, Stefano Roccella, Stefano Marco Maria De Rossi, Emanuele Cattin, Francesco Giovacchini, Fabrizio Vecchi, and Maria Chiara Carrozza. Neuroexos: A powered elbow exoskeleton for physical rehabilitation. *IEEE Transactions on Robotics*, 29(1):220–235, 2013.
- [10] Akshay Bhardwaj, Amir H Ghasemi, Yingshi Zheng, Huckleberry Febbo, Paramsothy Jayakumar, Tulga Ersal, Jeffrey L Stein, and R Brent Gillespie. Whos the boss? arbitrating control authority between a human driver and automation system. *Transportation Research Part F: Traffic Psychology and Behaviour*, 68:144–160, 2020.
- [11] Vahid Izadi, Arjun Yeravdekar, and Amirhossein Ghasemi. Determination of roles and interaction modes in a haptic shared control framework. In *ASME 2019 Dynamic Systems and Control Conference*. American Society of Mechanical Engineers Digital Collection, 2019.
- [12] R Brent Gillespie, M OModhrain, Philip Tang, David Zaretzky, and Cuong Pham. The virtual teacher. In *Proceedings of the ASME Dynamic Systems and Control Division*, volume 64, pages 171–178. American Society of Mechanical Engineers, 1998.
- [13] Douglas P Haanpaa and Gerald P Boston. An advanced haptic system for improving man-machine interfaces. *Computers & Graphics*, 21(4):443–449, 1997.
- [14] Shinsuk Park, Robert D Howe, and David F Torchiana. Virtual fixtures for robotic cardiac surgery. In *International Conference on Medical Image Computing and Computer-Assisted Intervention*, pages 1419–1420. Springer, 2001.
- [15] Ryojun Ikeura, Tomoki Moriguchi, and Kazuki Mizutani. Optimal variable impedance control for a robot and its application to lifting an object with a human. In *Proceedings. 11th IEEE International Workshop on Robot and Human Interactive Communication*, pages 500–505. IEEE, 2002.
- [16] Ryojun Ikeura, Akishi Morita, and Kazuki Mizutani. Variable damping characteristics in carrying an object by two humans. In *Proceedings 6th IEEE International Workshop on Robot and Human Communication. RO-MAN’97 SENDAI*, pages 130–134. IEEE, 1997.
- [17] Hirohiko Arai, Tomohito Takubo, Yasuo Hayashibara, and Kazuo Tanie. Human-robot cooperative manipulation using a virtual nonholonomic constraint. In *Proceedings 2000 ICRA. Millennium Conference. IEEE International Conference on Robotics and Automation. Symposia Proceedings (Cat. No. 00CH37065)*, volume 4, pages 4063–4069. IEEE, 2000.
- [18] Kyle B Reed and Michael A Peshkin. Physical collaboration of human-human and human-robot teams. *IEEE Transactions on Haptics*, 1(2):108–120, 2008.
- [19] Raphaela Groten, Daniela Feth, Harriet Goshy, Angelika Peer, David A Kenny, and Martin Buss. Experimental analysis of dominance in haptic collaboration. In *Robot and Human Interactive Communication, 2009. RO-MAN 2009. The 18th IEEE International Symposium on*, pages 723–729. IEEE, 2009.
- [20] Akshay Bhardwaj, Brent Gillespie, and James Freudenberg. Estimating rack force due to road slopes for electric power steering systems. In *2019 American Control Conference (ACC)*, pages 328–334. IEEE, 2019.
- [21] Bo Yu, R Brent Gillespie, James S Freudenberg, and Jeffrey A Cook. Human control strategies in pursuit tracking with a disturbance input. In *Decision and Control (CDC), 2014 IEEE 53rd Annual Conference on*, pages 3795–3800. IEEE, 2014.
- [22] Bo Yu, R Brent Gillespie, James S Freudenberg, and Jeffrey A Cook. Identification of human feedforward control in grasp and twist tasks. In *American Control Conference (ACC), 2014*, pages 2833–2838. IEEE, 2014.
- [23] Jeremy D Brown, Andrew Paek, Mashaal Syed, Marcia K OMalley, Patricia A Shewokis, Jose L Contreras-Vidal, Alicia J Davis, and R Brent Gillespie. An exploration of grip force regulation with a low-impedance myoelectric prosthesis featuring referred haptic feedback. *Journal of neuroengineering and rehabilitation*, 12(1):104, 2015.